Observation and description of phonon interactions in molecular dynamics simulations

A. J. H. McGaughey and M. Kaviany*
Department of Mechanical Engineering, University of Michigan, Ann Arbor, Michigan 48109-2125, USA
(Received 24 January 2005; published 26 May 2005)

Three-phonon interactions are identified and analyzed in nonequilibrium molecular dynamics simulations of the Lennard-Jones face-centered cubic crystal. The small simulation cells studied and the classical nature of the simulations lead to a different description of the phonon transport than the quantum-particle model. The selection process is strictly governed by the mode wave vectors. In determining the strength of an allowed interaction, one must consider the mode polarizations and frequencies—the latter in the context of internal resonance. The results are consistent with intrinsic scattering rates calculated directly from the Lennard-Jones potential.

DOI: 10.1103/PhysRevB.71.184305 PACS number(s): 63.20.Dj

I. INTRODUCTION

Results of molecular dynamics (MD) simulations of a face-centered cubic (fcc) Lennard-Jones (LJ) crystal have recently been used to parametrize a Boltzmann transport equation (BTE) formulation for predicting lattice thermal conductivity.[1] The specific heat, phonon dispersion, and phonon relaxation times were specified with no fitting parameters. Good agreement is found between the predicted thermal conductivities (based on an isotropic assumption) and results obtained by applying the Green-Kubo method to the same system. The finite relaxation times and thermal conductivities indicate that multiphonon interactions are present in the MD simulation cell. The frequency and temperature dependencies of these phonon relaxation times, however, were found to be inconsistent with standard forms used in the literature based on low frequency asymptotes (e.g., $1/\tau \propto \omega^n T^p$, where τ is the relaxation time, ω is frequency, T is temperature, and n and p are constants[2,3]). In Figs. 1(a) and 1(b), the inverse of the longitudinal and transverse relaxation times in the [100] direction, scaled for argon, are plotted as a function of frequency. The behavior cannot fit a function of the form ω^n. One or two such terms are required in each of two distinct regimes. In Fig. 1(c), the exponent p of the temperature-dependent fits of the data in Figs. 1(a) and 1(b) is shown as a function of the magnitude of the wave vector. A dimensionless wave vector, $\boldsymbol{\kappa}^*$, is defined as $\boldsymbol{\kappa}/(2\pi/a)$, where a is the conventional unit cell size, such that $\boldsymbol{\kappa}^*$ will vary between zero and one in the [100] direction of the Brillouin zone (BZ). There is significant variation. Classical phonon theory predicts a p value of unity at high temperature.[4]

Thus questions arise as to the nature of the relaxation time behavior. Why does the transverse curve in Fig. 1(b) turn down at high frequencies for low temperatures, but not for higher temperatures? Why do the longitudinal and transverse relaxation times become very similar (as a function of frequency) as the temperature increases? To answer these questions, the phonon interactions that cause the relaxation process must be examined. Identification and analysis of these interactions is the focus of this work. We begin with an introduction to the MD approach and a description of the system we will study. The nature of phonon transport in the MD system, and how this must be considered in a different manner than the quantum-particle approach, is then discussed. We then present three simulation methodologies that allow for the observation of phonon interactions. Nonequilibrium, unsteady, and steady-state approaches are considered. Evidence of phonon interactions is found, and interpreted in the context of both lattice dynamics and classical dynamics.

II. PHONON TRANSPORT IN MOLECULAR DYNAMICS SIMULATIONS

A. Molecular dynamics simulations

In an MD simulation, the position and momentum space trajectories of a system of classical particles are predicted using the Newton laws of motion and an appropriate interatomic potential. A benefit of MD simulations is the opportunity to make atomic-level observations not possible in experiments. One drawback is that quantum effects (e.g., electrons and the temperature dependence of phonon mode populations) are not considered. At sufficiently high temperatures and for many problems of interest, the classical-quantum difference is not a serious concern.

There is no simple way to explicitly include quantum effects in MD simulations. The intent of the simulations is, in fact, to save computational time by ignoring quantum effects. That being said, effort has been made to address this issue by mapping the results of MD simulations onto a quantum system using a temperature-scaling procedure. A drawback of this approach is that it maps the entire MD system onto a quantum description.[5] Quantum effects manifest on a mode-by-mode basis, making corrections on an integrated level unsuitable. This approach, when applied to thermal conductivity prediction, has had mixed results.[6–8] Li[5] suggests a way in which one can link the classical MD system to a quantum description through the BTE.

The MD simulations discussed here correspond to a 256-atom fcc LJ crystal. The use of a simple system allows for fast simulation runs and the elucidation of results difficult to resolve in more complex materials. No size effects have been found in thermal conductivities predictions for simulation cells with 256, 500, and 864 atoms.[1] We interpret this result as an indication that the small simulation cell contains

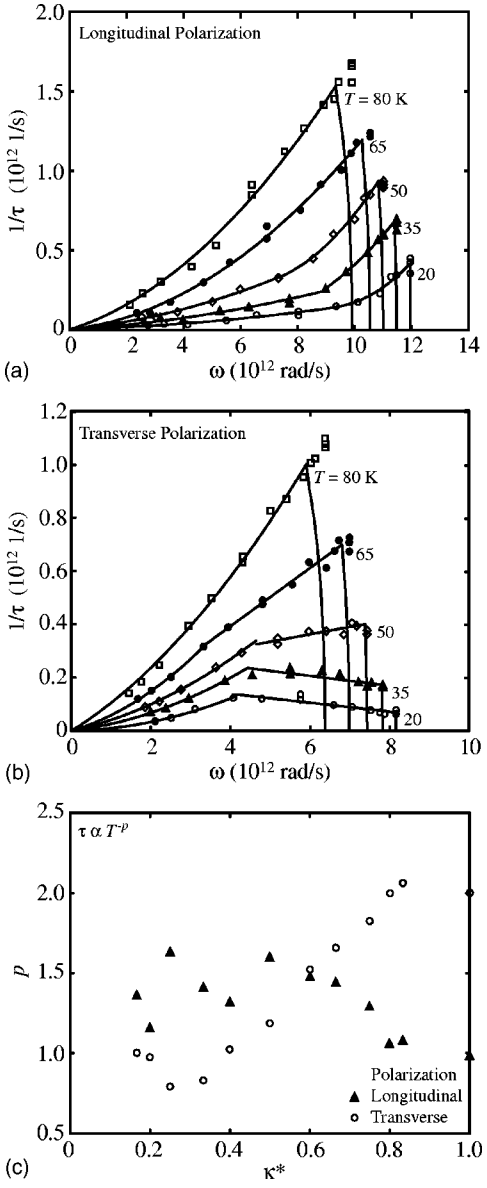

FIG. 1. Frequency dependence of the [100] relaxation times predicted from MD for the LJ argon fcc crystal in (a) the longitudinal polarization and (b) the transverse polarization (Ref. 1). (c) Temperature dependence of the data in (a) and (b).

enough phonon modes to establish representative phonon scattering. Results presented with dimensions are scaled for argon.[9] Simulations are run in the *NVE* (constant mass, volume, and energy) and *NVT* (constant mass, volume, and temperature) ensembles with a time step of 4.285 fs, and periodic boundary conditions are imposed in all directions. The simulation cell size is chosen so that the equilibrium system is at zero pressure. Further details of the simulation procedures are described elsewhere.[1,6,10]

B. Interaction selection rules

In a dielectric crystal, heat transfer is realized through atomic vibrations. In lattice dynamics theory,[4,9,11,12] a frequency space description is sought through which one can predict and analyze the motions of the atoms. Instead of discussing the localized motions of individual atoms, the system is described by energy waves (the normal modes) with a wave vector, a frequency, and a polarization vector ($\mathbf{e}$). In a finite crystal, the allowed modes are finite in number. The extent of these modes in the frequency space describes the BZ. The Appendix contains a review of the lattice dynamics concepts used here.

Phonon transport and interactions have traditionally been described in the context of a quantum-particle model. The existence of a particle implies localization. A phonon mode in a crystal is, in fact, completely nonlocalized. But, one can imagine that in a large system (where the resolution of the BZ is fine), a wave packet can be created by superimposing phonon modes of similar wavelengths. Such a wave packet, or phonon particle, can then move around the system. These phonon particles are assumed to propagate ballistically in between collisions with other phonons, impurities, and boundaries. Under these conditions, the phonon particles make up a phonon gas.

Interphonon interactions are the only form of scattering present in the MD system studied here. To model such interactions theoretically, one must consider third-order and higher (anharmonic) terms in the expansion of the lattice potential energy about its minimum. The third-order term, related to three-phonon interactions, is the basis for standard analysis techniques. The mathematics at this level are involved, and the level of complexity increases significantly for fourth-order and higher terms. These higher-order effects, however, are generally thought insignificant.[4]

In the three-phonon interaction formulation there are two types of allowed events. In a type I interaction, one phonon decays into two others. In a type II interaction, two phonons combine to form a third. To satisfy conservation of energy, phonon processes in which three phonons are either created or destroyed are not permitted. Two sets of selection rules exist for the allowed interactions.

First, from the translational invariance of the lattice potential energy, the wave vectors of the phonon modes in question must satisfy[4]

$$\boldsymbol{\kappa}_1 = \boldsymbol{\kappa}_2 + \boldsymbol{\kappa}_3 + \mathbf{G} \text{ (type I)}, \tag{1}$$

$$\boldsymbol{\kappa}_1 + \boldsymbol{\kappa}_2 = \boldsymbol{\kappa}_3 + \mathbf{G} \text{ (type II)}, \tag{2}$$

where $\mathbf{G}$ is either equal to zero [corresponding to a normal (N) process] or a reciprocal-lattice vector [corresponding to an Umklapp (U) process]. This criterion is valid in both the classical and quantum descriptions of the phonon system. These wave-vector selection rules are only dependent on the crystal structure, and are independent of temperature. By multiplying through by $\hbar$, the Planck constant divided by 2π, one obtains terms with the units of momentum, so that this criterion is often referred to as the conservation of crystal (or phonon) momentum. This is not real momentum, however, as no phonon modes (other than that at the center of the BZ) can carry physical momentum. Note that selection rules for the classical system cannot contain $\hbar$.

The second selection rule, only applicable to the quantum system, is based on conservation of energy. The second

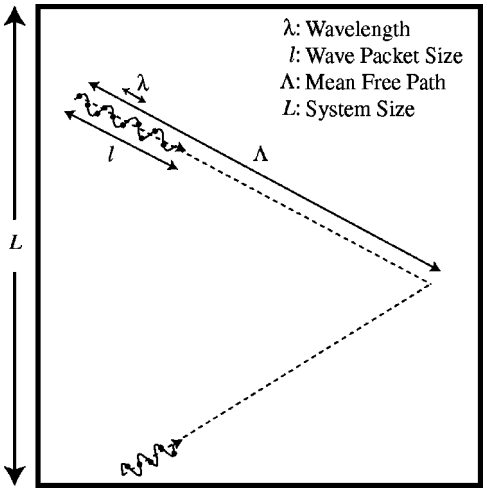

FIG. 2. Length scales in the phonon gas. For the phonon particle and phonon gas concepts to be valid, $\lambda \ll l \ll \Lambda \ll L$.

quantization in the formulation of the lattice dynamics theory results in the energy of the phonon modes being discretized into packets of size $\hbar\omega$. For the type I and II interactions, conservation of energy leads to[4]

$$\hbar\omega_1 = \hbar\omega_2 + \hbar\omega_3 \text{ (type I)}, \tag{3}$$

$$\hbar\omega_1 + \hbar\omega_2 = \hbar\omega_3 \text{ (type II)}. \tag{4}$$

In such calculations, one must use the true anharmonic mode frequencies.[6] The second quantization cannot be made in the MD system. Energy is still conserved in the *NVE* ensemble, but not as described by Eqs. (3) and (4). In the quantum-particle description, one assumes that the interactions occur instantaneously (i.e., they are discrete events). In the MD system the energy in a given mode is a continuous function of time, and discrete energy exchange events will not occur. One must instead think of a continuous flow of energy between the modes in the frequency space. Considered from another angle, the MD system is a nonlinear, many-body dynamics problem solved using the Newton laws of motion.

The selection rules only indicate what three-phonon interactions are possible (see Sec. IV). The rate at which an interaction takes place is related to the intrinsic scattering rate and to the degree of departure of the mode populations from the equilibrium distribution. The intrinsic scattering rate is considered in Sec. V.

C. Phonon gas and normal modes

To describe a phonon system as a phonon gas in which the particles interact weakly (i.e., kinetically), a number of criteria must be satisfied regarding the length scales in the system (see Fig. 2). To treat a phonon as a particle, a wave packet must be formed, whose size, l, is much greater than the wavelength, λ, of the mode of interest. For the wave packets to have distinct interactions with each other, the distance they travel between collisions (the average value of this distance is the mean free path, Λ) must be much greater than the size of the wave packets. And, if interphonon interactions are to dominate the phonon scattering (i.e., diffuse transport), the size of the system, L, must be much greater than the mean free path.

In the 256-atom LJ fcc crystal studied here, four points apart from the origin can be resolved in the [100] direction of the BZ. To form a wave packet, modes in the vicinity of the mode of interest are superimposed. This is clearly impossible in the MD system. Considered from a different viewpoint, the system is too small to form such a packet, as the side-length and all the available wavelengths are of a similar size. Very large MD system sizes are required to form a wave packet.[13–15]

Having established that a wave packet cannot be formed in an MD simulation cell with a few hundred atoms, the possibility of treating the system as a collection of phonon particles is eliminated. The phonon modes must thus be treated as they are defined in the lattice dynamics theory: completely nonlocalized. The energy within a given phonon mode, while corresponding to a point in frequency space, cannot be spatially resolved in real space.

If a phonon mode cannot be spatially resolved, the concept of the mean free path becomes questionable. It is better to think of the energy in a given mode in the context of a relaxation time. From the phonon particle perspective, the relaxation time is the average time between collisions. In the nonlocalized description, the relaxation time is an indication of the time scale over which the energy in a mode stays correlated with itself. That is, the time over which a certain percentage of the energy in a mode is the energy that was there initially, and not energy scattered into the mode as its original energy is scattered out to other modes.

III. DESCRIPTION OF THE FIRST BRILLOUIN ZONE

While we focus here on the 256-atom LJ fcc system, the calculations and analysis described are applicable to any size of simulation cell, crystal structure, or interatomic potential. A point in the BZ will be denoted by $(\kappa_x^*, \kappa_y^*, \kappa_z^*)$, and a normal mode will be denoted by both the point in the BZ and its polarization as $[(\kappa_x^*, \kappa_y^*, \kappa_z^*), (e_x, e_y, e_z)]$.

Including the boundaries, there are 341 distinct points in the BZ. For each point there are three modes (polarizations). Points on the surface of the BZ separated by a reciprocal lattice vector [here, appropriate rotations of (2, 0, 0) and (1, 1, 1)] are degenerate for calculation purposes. Two hundred and fifty six points are left after accounting for the degeneracies, which correspond to the 768 normal modes. This is expected for a system with 256 atoms, each of which has three positional degrees of freedom. The degenerate points are still of interest, however, as they can lead to different phonon scattering processes [i.e., the distinction between an *N* process and a *U* process; see Eqs. (1) and (2)].

In the calculation of the energy of a normal mode [see Eqs. (A3), (A4), and (A6)], there are terms of the form

$$\left| \sum_i m_i^{1/2} \exp(-i\boldsymbol{\kappa} \cdot \mathbf{r}_{i,o}) e_k^*(\boldsymbol{\kappa}, \nu) \cdot \mathbf{u}_i \right|^2 \tag{5}$$

and its derivative. Here, m_i is the mass of atom i, $\mathbf{r}_{i,o}$ is its equilibrium position, $\mathbf{u}_i$ is its displacement from equilibrium,

TABLE I. Symmetry reduced points in the 256-atom LJ fcc crystal MD simulation cell. The chosen points are in the first octant, and are listed in order of increasing wave vector magnitude.

(0.25, 0, 0), (0.25, 0.25, 0), (0.25, 0.25, 0.25),
(0.5, 0, 0), (0.5, 0.25, 0), (0.5, 0.25, 0.25),
(0.5, 0.5, 0), (0.75, 0, 0), (0.5, 0.5, 0.25),
(0.75, 0.5, 0), (0.75, 0.5, 0.25), (1, 0, 0),
(1, 0.25, 0), (0.75, 0.75, 0), (1, 0.5, 0)

ν describes the polarization of the normal mode, and * denotes the complex conjugate. These expressions are invariant to a switch from $\boldsymbol{\kappa}$ to $-\boldsymbol{\kappa}$. One can exploit this symmetry to reduce the number of computations required in the ensuing analysis.

In cases where mode interactions are not explicitly modeled,[1] the data associated with a set of points related by a rotation operation [e.g., (1, 0, 0), (0, 1, 0), and (0, 0, 1)] can be averaged. This is unsuitable for the simulations discussed here, other than for generating a general image of the BZ. Considering this criterion, and that described in the previous paragraph, 18 distinct points are left in the first octant of the BZ; they are listed in Table I. The origin is excluded, as this mode (which corresponds to rigid motion of the system) does not contribute to conduction heat transfer.

IV. NORMAL MODE INTERACTIONS

How does the energy in a normal mode cascade through the available frequency space? This question underlies phonon dynamics. Its answer is needed to understand phonon thermal transport at all length scales.

The ensuing analysis and discussion will focus on interactions involving three normal modes. To begin, we analyze an initially perturbed system as it relaxes to equilibrium. Then, we consider a continuously excited system, and end by investigating an equilibrium system. For consistency, most analysis is done with the mode [(0.5, 0, 0), (1, 0, 0)] at a temperature of 50 K.

A. Pulsed mode excitation: Unsteady system

Consider a system with the atoms at their equilibrium positions. One normal mode, $[\boldsymbol{\kappa}, \mathbf{e}]$, is then excited by perturbing the atomic positions according to[16,17]

$$\mathbf{r}_i(t=0) = \mathbf{r}_{i,o} + \alpha \mathbf{e}(\boldsymbol{\kappa}, \nu)\sin(\boldsymbol{\kappa} \cdot \mathbf{r}_{i,o}), \tag{6}$$

where $\mathbf{r}_i$ is the position of atom i, t is time, and α is a scalar to be specified. As discussed in Sec. III, this perturbation will equally excite the mode $[-\boldsymbol{\kappa}, \mathbf{e}]$. The system is then released and allowed to come to equilibrium in the *NVE* ensemble. This is similar to pulling the mass in a mass-spring system away from equilibrium and releasing it. If the initial velocities are set to zero, the system will oscillate in the excited mode indefinitely; it is in a metastable equilibrium state. To induce relaxation, but not bias it, an extremely small, random velocity is given to each of the particles (equivalent to a temperature on the order of 10^{-18} K). This small perturbation is sufficient to break the system out of the metastable equilibrium state within about 10^4 time steps. No significant qualitative differences are found when starting from different initial conditions. Using finite velocities as an initial condition is undesirable. Doing so leads to the activation of numerous modes due to the forced motion of the atoms.

During the relaxation from the initial condition to equilibrium, the frequency space energy is monitored on a mode-by-mode basis. Three distinct temporal phases are observed. Initially, all the energy stays in the excited mode and oscillates between kinetic energy and potential energy. Eventually, the small initial velocities grow, and cause the initially excited mode to decay. When this happens, only a few modes are activated. In time, more and more modes are activated, and the system eventually reaches equilibrium. It is in the short time after the initially excited mode starts to decay that one can extract useful data.

This approach is similar to one used to investigate phonon transport across material interfaces.[13,14] In that work, a wave packet is created in a silicon simulation cell thousands of atoms long and allowed to propagate spatially. Atoms outside of the wave packet are initially taken to be at rest. This approach was later used to look at phonon mode decay in silicon.[15] The main difference between those simulations and the ones discussed here is the spatial localization achieved in their large simulation cells, compared to the nonlocalized behavior we study.

A typical result for the mode [(0.5, 0, 0), (1, 0, 0)] is shown in Fig. 3(a). The normal mode energies are scaled by the expectation value of the total energy of the associated classical-harmonic system, $3(N-1)k_BT$. The value of α (0.082) is chosen so that the equilibrium temperature is 20 K. Because of the harmonic nature of the normal mode calculations, the phonon space energy is not conserved except for very small values of α. Plotted in Fig. 3(a) are the energies of the initially excited mode and two of the modes that show a significant activation after the decay begins. The wave vectors of these two modes, (0.5, 0, 0.25) and (0, 0, −0.25), together with that of the initially excited mode, [(0.5, 0, 0)], satisfy Eq. (1) with $\mathbf{G}=0$, indicating that the decay corresponds to a type I *N* process. Additional interactions of this type related to appropriate rotations of (0.5, 0, 0.25) and (0, 0, −0.25) are also observed. The instantaneous temperature of the system is shown in the inset of Fig. 3(a). In the initial regime, before the decay has occurred, the temperature fluctuates between 0 K and 40 K. The system alternates between states with either all potential energy or all kinetic energy. Once the decay begins, the fluctuations decrease.

One does not always find the well-defined behavior seen in Fig. 3(a). Sometimes multiple modes are excited in the initial, predecay regime. This occurs for the mode [(0.25, 0, 0), (1, 0, 0)], as shown in Fig. 3(b). While not present at $t=0$, the modes [(0.5, 0, 0), (1, 0, 0)] and [(0.75, 0, 0), (1, 0, 0)] become active before the decay occurs. This is evident from both the time-history of the mode energies, which show a regular, periodic behavior, and the system temperature, shown in the inset of Fig. 3(b). When the decay begins, the modes corresponding to the decay of [(0.5, 0, 0), (1, 0, 0)] are observed, as shown in Fig. 3(b). Thus, it will be difficult

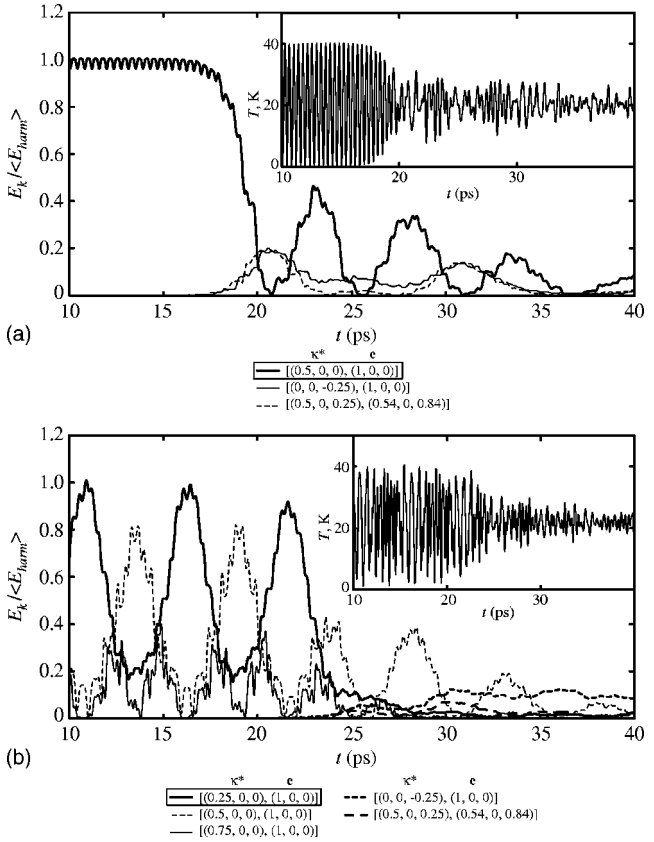

FIG. 3. Relaxation of the MD system when one mode is initially excited and all others are unperturbed. The plots correspond to initial excitations of the modes (a) [(0.5, 0, 0), (1, 0, 0)] (α=0.082) and (b) [(0.25, 0, 0), (1, 0, 0)] (α=0.16). In both parts of the figure, the instantaneous system temperature is shown in the inset plot.

to extract useful information from the modes activated during the decay, as their origins may be unclear. This phenomenon occurs because the MD system is anharmonic. The atoms exert nonlinear forces on each other in three dimensions, and so do not follow sinusoidal trajectories. When certain modes are initially excited, other modes are also excited in the resulting motion of the atoms, without a decay to equilibrium.

The most significant drawback of this approach, and that which spatially localizes the phonon mode,[13–15] is temperature-related. The amount of energy in the system is a function of the size of the initial perturbation, controlled by the parameter α. By assuming an equipartition of energy, the temperature of the final, equilibrium system can be approximated from the initial condition. To reach higher temperatures, one must apply larger perturbations. For larger perturbations, the system will become more anharmonic before the decay. In this regime, the suitability of the normal mode energy calculation will be questionable. Also, as seen in the insets of Figs. 3(a) and 3(b), the temperature is not well-defined before equilibrium is reached. A possible solution is to perform such simulations in the *NVT* ensemble. The necessary modifications to the equations of motion, however, will result in the activation of undesirable modes, and a masking of the dynamics of interest.

Another issue with this procedure is that it will produce only type I interactions. To observe type II interactions, two modes would need to be initially excited, which would become an extensive numerical task. And, based on the possibility of exciting more than one mode from a given initial condition, it might be difficult to extract useful data. Nevertheless, these simulations are helpful since they have supplied a direct indication that three-mode interactions are taking place in the MD system.

B. Continuous mode excitation: Steady, nonequilibrium system

1. Concept

From an analysis standpoint, the simulations described in Sec. IV A are challenging because the temperature is poorly-defined, and extracting useful, quantitative information is difficult. As an alternative to initially exciting a mode and observing its decay, energy can be continuously added to a mode and allowed to dissipate. The steady nature of such an approach allows one to perform time averaging. The setup is somewhat analogous to a real system excited by a continuous monochromatic source of external radiation (e.g., photons).

To add energy to a normal mode, $[\boldsymbol{\kappa}, \mathbf{e}]$, the positions and momenta of all atoms are adjusted at every time step according to

$$\mathbf{r}_i(t)^{\text{new}} = \mathbf{r}_i(t)^{\text{old}} + \alpha \mathbf{e}(\boldsymbol{\kappa}, \nu)\sin[\boldsymbol{\kappa} \cdot \mathbf{r}_{i,o} - \omega(\boldsymbol{\kappa}, \nu)t], \quad (7)$$

$$\mathbf{p}_i(t - \Delta t/2)^{\text{new}} = \mathbf{p}_i(t - \Delta t/2)^{\text{old}} - \alpha\omega(\boldsymbol{\kappa}, \nu)\mathbf{e}(\boldsymbol{\kappa}, \nu) \times \cos[\boldsymbol{\kappa} \cdot \mathbf{r}_{i,o} - \omega(\boldsymbol{\kappa}, \nu)(t - \Delta t/2)], \quad (8)$$

in addition to the standard integration of the equations of motion. A given mode shape is superimposed onto the position and momentum space trajectories of the atoms. Though similar to the excitation prescribed by Eq. (6), this perturbation is time-dependent, and the momenta are also affected. The positions and momenta are offset by a half time-step as the Verlet leapfrog algorithm is used to integrate the equations of motion. Simulations were also performed where the force (i.e., the acceleration) on each atom was perturbed. Results similar to those here were found. The values of the perturbation parameter α to be studied are less than 10^{-4}, two orders of magnitude smaller than those used in the unsteady excitations of Sec. IV A. As a result, large anharmonic effects are not expected.

To allow the energy added to the system to dissipate, the simulations are run in the *NVT* ensemble. Although undesirable for the unsteady simulations described in Sec. IV A, we do not believe it is a critical factor here as the system is steady. The presented data correspond to the average of five sets of 2×10^5 time steps of MD simulation differentiated by random initial momenta. This time interval is preceded by 10^5 time steps of equilibration.

2. Results

The first step in the analysis consists of calculating the average energy, E_k, in each of the $3(N-1)$ modes, then scaling it by the value it takes on in the unperturbed *NVE* sys-

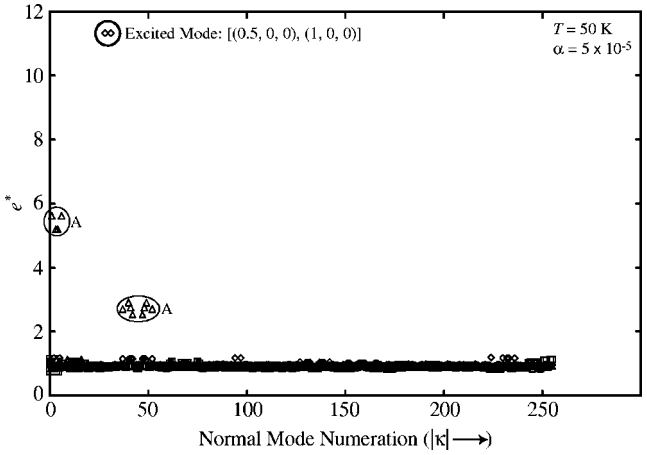

FIG. 4. Scaled energies for a continuous excitation of the mode [(0.5, 0, 0), (1, 0, 0)] at a temperature of 50 K. The value of the perturbation parameter α is 5×10^{-5}. Groups of points that are circled and labeled correspond to a part of a three-mode interaction. These are listed in Tables II and III. See also Figs. 5(a) and 5(b).

tem. This quantity, denoted hence by $e^*[\equiv E_k(\alpha)/E_k(\alpha=0)]$, indicates the extent of a given mode's enhancement or diminishment as a result of the perturbation. Results for the mode [(0.5, 0, 0), (1, 0, 0)] at a temperature of 50 K are shown in Figs. 4, 5(a), and 5(b). The horizontal axis in these figures is organized by an enumeration of the points in the BZ based on the magnitude of the wave vector, and goes from 0 to 255. At each unit, three points (i.e., modes) are plotted (one for each of the polarizations). In Fig. 4, the results for all points are shown. In Figs. 5(a) and 5(b), smaller portions of the overall picture are shown with a reduced vertical scale. The data correspond to an α value of 5×10^{-5}.

The data can be classified into three distinct groups. First, the excited mode, which shows up as two points, [(0.5, 0, 0), (1, 0, 0)] and [(−0.5, 0, 0), (1, 0, 0)], due to the symmetry of the BZ. It is clearly excited beyond its normal level. Most of the modes fall into an e^* range of 0.85 to 0.95. These modes are unaffected by the perturbation. The values of e^* are not unity (as they would be for $\alpha=0$), because the total system energy is not significantly different from its value in the equilibrium system.[6] The energy has been redistributed with some modes having very large values. The remaining modes have e^* values less than that of the excited mode, but are distinct from the nonexcited modes. These, the modes of greatest interest, will be referred to as the "activated modes." In Figs. 4, 5(a), and 5(b), some of these are grouped together based on the symmetry of their wave vectors and polarizations. There are two outlined areas for each of the letters A

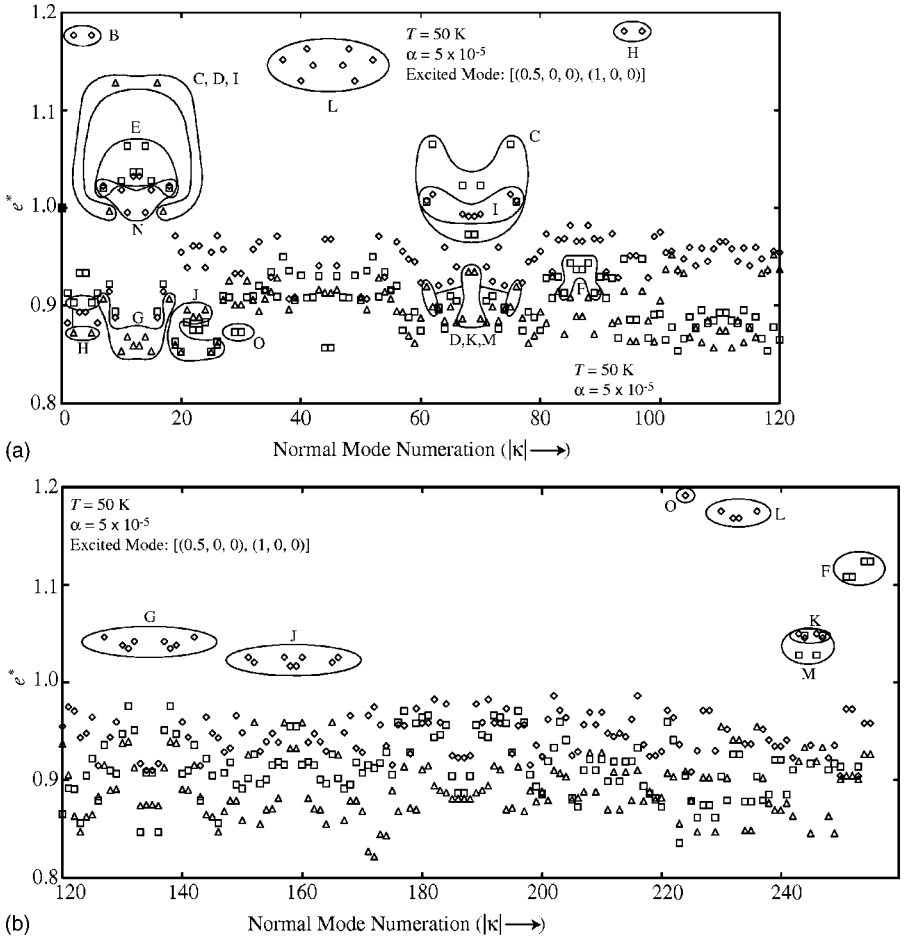

FIG. 5. The modes in Fig. 4 shown with a reduced vertical scale and an expanded horizontal scale: (a) modes 0–120 and (b) modes 120–255.

TABLE II. Three-mode interactions extracted from Figs. 4, 5(a), and 5(b). Mode 1 is [(0.5, 0, 0), (1, 0, 0)] and $\omega_1^*=15.90$. All interactions listed have $\delta\omega^*<0.1$, and are listed as if they were type I.

	Mode 2	Mode 3	Type/process	ω_2^*	ω_3^*	$a_1,a_2,a_3/O$	$\delta\omega^*$
A	[(0.5, 0, 0.25), (−0.54, 0, 0.84)]	[(0, 0, −0.25), (1, 0, 0)]	I *N*	9.78	5.83	1, −1, −1 3	0.018
B	[(0.25, 0, 0), (1, 0, 0)]	[(0.25, 0, 0), (1, 0, 0)]	I *N*	8.06	8.06	1, −1, −1 3	0.013
C	[(0.5, 0.25, 0.25), (0, −0.71, 0.71)]	[(0, −0.25, −0.25), (0, 0.71, −0.71)]	I *N*	10.72	4.96	1, −1, −1 3	0.013
D	[(0.5, 0.25, 0.25), (−0.72, 0.49, 0.49)]	[(0, −0.25, −0.25), (0, 0.71, −0.71)]	I/II *N*	10.65	4.96	1, −1, −1 3	0.018
E	[(0.25, 0, 0.25), (0, 1, 0)]	[(0.25, 0, −0.25), (0, 1, 0)]	I *N*	8.46	8.46	1, −1, −1 3	0.064
F	[(−0.5, 0, 0.5), (0, 1, 0)]	[(1, 0, −0.5), (0, 0, 1)]	I/II *N*/*U*	16.21	15.55	2, −1, −1 4	0.022
G	[(−0.25, 0, −0.25), (−0.71, 0, 0.71)]	[(0.75, 0, 0.25), (0.95, 0, 0.30)]	I/II *N*	4.96	21.08	1, 1, −1 3	0.014
H	[(−0.25, 0, 0), (0, 0, 1)]	[(0.75, 0, 0), (1, 0, 0)]	I/II *N*	5.84	21.33	1, 1, −1 3	0.025
I	[(0, −0.25, −0.25), (0, 0.71, −0.71)]	[(0.5, 0.25, 0.25), (0.69, 0.51, 0.51)]	I *N*	4.96	20.20	1, 1, −1 3	0.041
J	[(−0.25, −0.25, −0.25), (−0.82, 0.41, 0.41)]	[(0.75, 0.25, 0.25), (0.81, 0.41, 0.41)]	I/II *N*	7.11	21.46	1, 1, −1 3	0.098
K	[(−0.5, −0.25, −0.25), (−0.72, −0.49, −0.49)]	[(1, 0.25, 0.25), (1, 0, 0)]	I/II *N*/*U*	10.65	21.13	2, −1, −1 4	0.018

and C–O, representing pairs of modes that, together with the excited mode, form a three-mode interaction. For B, the identified mode interacts with itself. Representative pairings (i.e., not including all possible combinations based on permutations) are listed in Tables II and III. Note that interaction A is the same as that observed for the unsteady simulations discussed in Sec. IV A, and shown in Fig. 3(a).

Some of the observed type I interactions have a small, but nonzero, value of the quantity $(\omega_1-\omega_2-\omega_3)/\omega_1$. This is an indication of the presence of internal resonance, a concept that can be used to describe mode interactions in a nonlinear dynamical system.[18] In general, interactions that satisfy

$$a_1\omega_1 + a_2\omega_2 + a_3\omega_3 + \cdots + a_n\omega_n \approx 0,$$

$$a_1,a_2,a_3,\ldots,a_n = \cdots -2,-1,1,2,\ldots, \tag{9}$$

are possible. One seeks linear combinations of the system frequencies and their harmonics (through a_n values with a magnitude greater than unity) that sum to zero. Because Eq. (9) is not an equality, internal resonance is not a selection rule, but a guideline to suggest what processes can occur. Also, note that the internal resonance concept is not related to conservation of energy [see Eqs. (3) and (4)]. The linear combination of the frequencies (based on the a_n values) need

TABLE III. Three-mode interactions extracted from Figs. 4, 5(a), and 5(b). Mode 1 is [(0.5, 0, 0), (1, 0, 0)] and $\omega_1^*=15.90$. All interactions listed have $\delta\omega^*>0.1$, and are listed as if they were type I.

	Mode 2	Mode 3	Type/process	ω_2^*	ω_3^*	$a_1,a_2,a_3/O$	$\delta\omega^*$
L	[(−0.5, 0, 0.25), (0.84, 0, −0.54)]	[(1, 0, −0.25), (1, 0, 0)]	I *N*/*U*	17.58	22.18	1, 1, −1 3	0.711
M	[(−0.5, −0.25, −0.25), (−0.72, 0.49, 0.49)]	[(1, 0.25, 0.25), (0, 0.71, 0.71)]	I *N*/*U*	10.65	18.40	1, 1, −1 3	0.512
N	[(0.25, −0.25, 0), (0.71, −0.71, 0)]	[(0.25, 0.25, 0), (0.71, 0.71, 0)]	I *N*	12.58	12.58	1, −1, −1 3	0.583
O	[(−0.5, 0, 0), (0, 0, 1)]	[(1, 0, 0), (1, 0, 0)]	I/II *N*/*U*	11.26	23.40	1, −1, −1 3	0.528

not match that for the wave vectors. For the purposes of this investigation, the analysis is restricted to the case of $n=3$ (i.e., three-mode interactions). The frequency residual, $\delta\omega^*$, is defined as

$$\delta\omega^* = \left| \frac{a_1\omega_1 + a_2\omega_2 + a_3\omega_3}{\omega_1} \right|, \tag{10}$$

and the order of the interaction, O, is defined as

$$O = \sum_n |a_n|. \tag{11}$$

For each set of three modes listed in Tables II and III, the minimum value of the frequency residual is obtained by considering processes with O values of three or four (i.e., one of the a_n values can be equal to two). Interactions with $\delta\omega^*$ less than 0.1 are listed in Table II, and those with values greater than 0.1 are listed in Table III.

Simply based on the groupings A–O, and not by the e^* values, one cannot make a distinction between type I and type II interactions. For every type I interaction

$$\boldsymbol{\kappa}_1 = \boldsymbol{\kappa}_2 + \boldsymbol{\kappa}_3 + \mathbf{G},$$

there is a type II interaction

$$\boldsymbol{\kappa}_1 + (-\boldsymbol{\kappa}_2) = \boldsymbol{\kappa}_3 + \mathbf{G}.$$

As the modes $\boldsymbol{\kappa}_2$ and $-\boldsymbol{\kappa}_2$ are not distinguishable in the simulations, neither are these two processes. The frequency residual will also be the same, as the coefficients in Eq. (9) can take on negative values.

The distinction between a type I and a type II interaction can be resolved in some cases by considering the e^* values. For example, with interaction A, both modes 2 and 3 have an e^* value greater than unity, indicating they are both activated in a type I interaction. For those interactions where only one of the modes is clearly activated (e.g., F), both type I and type II interactions are noted in Tables II and III. The apparent nonexcitation of a mode may be a result of it taking part in both type I and type II interactions, effects of which could have a cancelling effect on e^*.

For any interaction that involves a point on the surface of the BZ (e.g., F), the distinction between N and U processes is ambiguous. For example, if in the interaction

$$\boldsymbol{\kappa}_1 = \boldsymbol{\kappa}_2 + \boldsymbol{\kappa}_3,$$

mode 3 is on the surface, then there exists a degenerate mode 4 given by

$$\boldsymbol{\kappa}_4 = \boldsymbol{\kappa}_3 + \mathbf{G},$$

such that

$$\boldsymbol{\kappa}_1 = \boldsymbol{\kappa}_2 + \boldsymbol{\kappa}_4 + \mathbf{G}$$

is satisfied. As modes 3 and 4 are degenerate, these two processes are not distinguishable. These cases are indicated in Tables II and III.

For the interactions listed in Table II, the value of $\delta\omega^*$ is small (<0.1), and the internal resonance argument seems reasonable. For interactions L through O, the frequency residual is large, casting doubt on whether or not these interactions are happening. There are a number of possible explanations for the appearance of large e^* values for the associated modes. A higher-order description (both in terms of O and the number of modes considered) may be necessary. The observed activation may also result from the decay of activated modes, and not the excited mode (i.e., a secondary effect). Finally, as seen in the unsteady, pulsed excitation in Sec. IV A, some modes may be immediately excited by the continuous excitation, and not as a result of the excited mode's decay.

The frequency residual is a good gauge of whether or not an interaction will occur. But, it is not sufficient. For example, the value of $\delta\omega^*$ for interaction A, but with a polarization of (0, 1, 0) for mode 3, is the same as that listed in Table II. Yet, this mode is not activated. As given, the polarization vectors all lie in the same plane. If the polarization of mode 3 is changed to (0, 1, 0), the polarizations are no longer planar. It appears that interactions are selected in which the atoms vibrate in a direction near to that of the original mode. A similar effect is found with the wave vectors. By combining the frequency, polarization, and wave vector criteria, one can get a better idea of what modes are activated by a given excitation. To this end, an objective function g^* is defined as

$$g^* = \delta\omega^* + \frac{2 - |\mathbf{e}_1 \cdot \mathbf{e}_2| - |\mathbf{e}_2 \cdot \mathbf{e}_3|}{2} + \frac{2 - \dfrac{|\boldsymbol{\kappa}_1 \cdot \boldsymbol{\kappa}_2|}{|\boldsymbol{\kappa}_1||\boldsymbol{\kappa}_2|} - \dfrac{|\boldsymbol{\kappa}_1 \cdot \boldsymbol{\kappa}_3|}{|\boldsymbol{\kappa}_1||\boldsymbol{\kappa}_3|}}{2}. \tag{12}$$

A small value of g^* seems to be a sufficient, but not necessary, condition for the observation of an interaction. To this point, we have not identified definitive criteria that can predict what modes will be activated, and to what extent. Ideally, one would be able to make such a prediction without running a simulation, based simply on the frequency space characteristics of the material.

Similar simulations were run for all other modes and polarizations in the [100] direction. In some cases, the nature of the results is similar to that for [(0.5, 0, 0), (1, 0, 0)], but in others, little interesting behavior is found (i.e., it is difficult to distinguish between the activated modes and the unaffected modes). This likely indicates that there are certain decay paths that dominate for some modes, while for others the effects are spread more evenly amongst the hundreds of possible interactions.

Additional technical details regarding the nonequilibrium simulations, including a discussion of the effects of changing the size of the perturbation, the frequency of excitation, the thermostat time constant, and the temperature, are presented elsewhere.[6] The results at temperatures of 20 K and 80 K for [(0.5, 0, 0), (1, 0, 0)] are in qualitative agreement with those at a temperature of 50 K presented here. At an equivalent perturbation level (giving an excited mode e^* of around ten), similar modes are activated, albeit at different levels. Due to the sensitive nature of the system response, quantitative comparisons are challenging to make. These differences are likely responsible for the temperature dependence of the relaxation times [see Figs. 1(a) and 1(b)].

V. INTRINSIC SCATTERING RATE

The simulations discussed in Sec. IV deal with systems away from equilibrium. Three-mode interactions were observed, and some insight gained into why certain interactions occur, while others do not. The thermal conductivities predicted by the GK and BTE methods, however, are based on data from equilibrium simulations. As the value of the perturbation parameter α from the simulations of Sec. IV B goes to zero, it becomes difficult to resolve specific interactions.[6] And yet, it is the isolation of these effects at equilibrium that is crucial for understanding behaviors such as the relaxation-time curves shown in Fig. 1. A framework is sought that is as specific as possible, with minimal integration over time, space, modes, etc., as is done in the Green-Kubo and BTE approaches. Correlations that take multiple modes into account will likely be necessary [i.e., quantities based on one mode (such as e^*) are not enough]. In this section, calculations for the LJ system near equilibrium are presented.

In the scattering term in the BTE, the strength of a given interaction is a function of two effects: the intrinsic scattering rate, β, and the deviation of the mode populations from equilibrium. The intrinsic scattering rate for a three-mode interaction is given by[19]

$$\beta_{\nu_1,\nu_2,\nu_3}(\boldsymbol{\kappa}_1,\boldsymbol{\kappa}_2,\boldsymbol{\kappa}_3) = \frac{\pi\hbar}{4\rho^3 V^2 \omega_1\omega_2\omega_3}\left|\sum_{i,j,k}\sum_{\alpha,\beta,\gamma}\frac{\partial^3\Phi}{\partial u_{i,\alpha}\,\partial u_{j,\beta}\,\partial u_{k,\gamma}}\right|_0 \times e_\alpha^{\boldsymbol{\kappa}_1,\nu_1} e_\beta^{\boldsymbol{\kappa}_2,\nu_2} e_\gamma^{\boldsymbol{\kappa}_3,\nu_3}\exp[i(\boldsymbol{\kappa}_1\cdot\mathbf{r}_{o,i}+\boldsymbol{\kappa}_2\cdot\mathbf{r}_{o,j}+\boldsymbol{\kappa}_3\cdot\mathbf{r}_{o,k})]\Bigg|^2, \tag{13}$$

where ρ is the mass density. The first triple sum is over the atoms in the system. The second triple sum is over the x, y, and z directions. This expression is valid in both the classical and quantum systems for deviations not far from equilibrium. The third order derivative is also seen in Eq. (A1).[20] The intrinsic scattering rate is a function of the system properties, and is not related to the dynamics of a particular situation. Its value indicates the probability that an interaction will take place, and is readily calculated.

In Fig. 6, the intrinsic scattering rate is plotted as a function of the objective function g^* [see Eq. (12)] for all interactions involving [(0.5, 0, 0), (1, 0, 0)] as mode 1 at a temperature of 50 K in the 256-atom LJ fcc crystal. Anharmonic mode frequencies are used in the calculations.[6] While one could make some distinction between type I and type II interactions in the unsteady simulations of Sec. IV B by considering the e^* values, this is not possible here. As such, only the type II interactions are shown in the plot.

Of the 2286 interactions plotted in Fig. 6, 8.2% have a β value of more than 7.92×10^{11} 1/s, while 73.7% of the values are less than 1.58×10^{11} 1/s. The scattering rates are of the same order as the inverse relaxation times plotted in Figs. 1(a) and 1(b). The data points corresponding to interactions A–O listed in Tables II and III are indicated in the plot for those cases where $\beta > 1.58\times10^{11}$ 1/s. The only interactions that meet this criterion are from Table II. These interactions also have small values of the frequency residual, making them more likely to occur in the context of internal resonance. The presence of these modes is a sign that some behavior observed away from equilibrium is also present near equilibrium. Modes not seen previously are also present. Different weightings of the three terms in the objective function were investigated, but no combination suggests a strong correlation between β and g^*. Similar results have been found for the other modes and polarizations in the [100] direction.

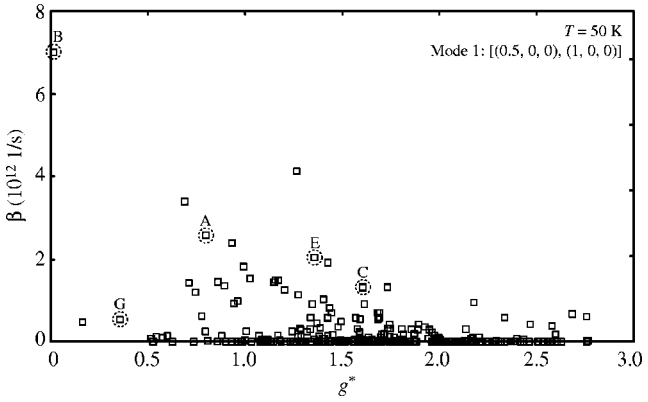

FIG. 6. The intrinsic scattering rate for interactions involving [(0.5, 0, 0), (1, 0, 0)] as mode 1 at a temperature of 50 K. The data are plotted against the objective function g^*, defined in Eq. (12), which contains information related to the mode frequencies, polarizations, and wave vectors. The interactions from Tables II and III that have a β value greater than 1.58×10^{11} 1/s are identified.

VI. SUMMARY

As discussed in Sec. II, the nature of phonon transport in an MD system with a few hundred or thousand atoms is different from that in a particle-based description. This does not mean, however, that large differences should be expected between predictions from a quantum model and from MD simulations. Treating a system as a phonon gas is merely one approach convenient for both formulation and interpretation. This model, however, is limited, because it cannot take interference effects into account, or consider small systems. The energy exchange between modes does not need to be considered as such, however. The nonlocalized description is actually a more general way of approaching the problem, which could also be applied to the quantum system. When addressing the issue of phonon transport in the MD system, one should seek a way to interpret the results of MD simulations and those from a quantum-particle model within a consistent framework, and not necessarily as one in the context of the other.

The exchange of energy between normal modes underlies all discussion of phonon thermal transport behavior. Without a fundamental knowledge of the nature of the transport, it may not be possible to understand how a complex crystal structure localizes energy, or to design a material with a specified thermal conductivity, or to interpret the shapes of relaxation-time curves. To date, work in molecular simulation and thermal transport seems to have skirted this issue

entirely.[6] While phonons are often mentioned, little effort has been taken to observe them, or to investigate how energy flows in a frequency space whose discretization cannot be ignored.

We have attempted to develop an understanding of how energy is transferred in the phonon space of the MD system. In the unsteady simulations of Sec. IV A, the decay of one normal mode into two others was directly observed. In the steady, nonequilibrium simulations of Sec. IV B, the multiple decay paths of a continuously excited mode were determined by looking at data averaged over a long simulation. The concept of internal resonance matched the behavior of the MD system well. The difficulty in distinguishing between type I and type II interactions, and *N* and *U* processes, was identified. In Sec. V, the intrinsic scattering rate was calculated from the interatomic potential, and some consistent results were found when compared to the interactions observed in Sec. IV. While the existence of three-mode interactions in the MD simulations has been clearly established, there is still much to be understood. In particular, the resolution of important behavior in the equilibrium system is a challenge. One would like to be able to predict what interactions will dominate in a material for a given set of conditions. While some guidelines were suggested (e.g., the objective function g^*), deeper investigation is required. One may need to develop three-mode correlation functions to see the desired behavior and obtain dynamical information.

ACKNOWLEDGMENTS

This work was supported by the U.S. Department of Energy, Office of Basic Energy Sciences under Grant No. DE-FG02-00ER45851, and the Horace H. Rackham School of Graduate Studies at the University of Michigan (A.J.H.M.).

APPENDIX: PHONON SPACE ANALYSIS

One of the foundations of phonon analysis is the harmonic approximation (i.e., that the phonon modes are equivalent to independent harmonic oscillators). Even when anharmonicities are taken into account, it is usually as a perturbation to the harmonic solution of the lattice dynamics problem. In these cases, phonon-phonon interactions are modeled as instantaneous events, preceded and followed by the independent propagation of phonons through the system (i.e., the phonons behave harmonically except when they are interacting).

At zero temperature in a classical solid, all the atoms are at rest in their equilibrium positions. The potential energy of the system, which is only a function of the atomic positions, can only take on one value (i.e., the phase space consists of a single point). As the temperature of the system is raised, the atoms move, and the extent of the associated phase space increases. Suppose that the equilibrium potential energy of a system with *N* atoms is given by Φ_0. If each atom *i* is moved by an amount $\mathbf{u}_i$, the resulting energy of the system, Φ, can be found by expanding around the equilibrium energy with a Taylor series as

$$\Phi = \Phi_0 + \sum_i \sum_\alpha \left.\frac{\partial \Phi}{\partial u_{i,\alpha}}\right|_0 u_{i,\alpha} + \frac{1}{2}\sum_{i,j}\sum_{\alpha,\beta} \left.\frac{\partial^2 \Phi}{\partial u_{i,\alpha}\partial u_{j,\beta}}\right|_0 u_{i,\alpha}u_{j,\beta} + \frac{1}{6}\sum_{i,j,k}\sum_{\alpha,\beta,\gamma} \left.\frac{\partial^3 \Phi}{\partial u_{i,\alpha}\partial u_{j,\beta}\partial u_{k,\gamma}}\right|_0 u_{i,\alpha}u_{j,\beta}u_{k,\gamma} + \cdots . \quad \text{(A1)}$$

Here, the i, j, and k sums are over the atoms in the system, and the α, β, and γ sums are over the x, y, and z directions. The first derivative of the potential energy with respect to each of the atomic positions is the negative of the net force acting on that atom. Evaluated at equilibrium, this term is zero. The first non-negligible term in the expansion is thus the second order term. The harmonic approximation is made by truncating the Taylor series after this term.

The harmonic approximation is valid for small displacements ($u_{i,\alpha} \ll r_{nn}$, the equilibrium atomic separation) about the zero-temperature minimum. Raising the temperature will cause deviations for two reasons. First, as the temperature increases, the displacements of the atoms will increase beyond what might be considered small. Second, the lattice constant will change, so that the equilibrium separation does not correspond to the well minimum. In the LJ argon system, the ratio $u_{i,\alpha}/r_{nn}$ reaches a value of 0.05 near a temperature of 20 K.[6] In order to deal with phonons and normal modes, however, the harmonic approximation is necessary. It is important to remember that this assumption underlies much of the presented analysis.

One of the challenges in working with Eq. (A1) under the harmonic approximation is the coupling of the atomic coordinates in the second-order derivatives. A transformation exists on the 3*N* real space coordinates (three for each of the *N* atoms) to a set of 3*N* new coordinates S_k (the normal modes) such that[12]

$$\Phi - \Phi_0 = \frac{1}{2}\sum_{i,j}\sum_{\alpha,\beta} \left.\frac{\partial^2 \Phi}{\partial u_{i,\alpha}\partial u_{j,\beta}}\right|_0 u_{i,\alpha}u_{j,\beta} = \frac{1}{2}\sum_k \left.\frac{\partial \Phi^2}{\partial S_k^2}\right|_0 S_k^* S_k, \quad \text{(A2)}$$

where

$$S_k(\boldsymbol{\kappa},\nu) = N^{-1/2}\sum_i m_i^{1/2}\exp(-i\boldsymbol{\kappa}\cdot\mathbf{r}_{i,o})\mathbf{e}_k^*(\boldsymbol{\kappa},\nu)\cdot\mathbf{u}_i. \quad \text{(A3)}$$

The normal modes are equivalent to harmonic oscillators, each of which has an associated wave vector, frequency, and polarization. They are completely nonlocalized spatially. The wave vectors can be determined from the crystal structure, and indicate the size and resolution of the associated BZ. The frequencies and polarizations are obtained from lattice dynamics calculations.

Starting from Eq. (A2), and noting that the second derivative terms can be considered as the spring constants, K_k, of the harmonic oscillators, the energy of one normal mode can be expressed as

$$\Phi_k = \frac{1}{2}\left.\frac{\partial \Phi^2}{\partial S_k^2}\right|_0 S_k^* S_k = \frac{1}{2}\frac{K_k}{m_k}S_k^* S_k = \frac{1}{2}\omega_k^2 S_k^* S_k, \quad \text{(A4)}$$

as the mass, frequency, and spring constant are related through $\omega_k = (K_k/m_k)^{1/2}$. The average potential energy will be

$$\langle \Phi_k \rangle = \frac{1}{2}\omega_k^2 \langle S_k^* S_k \rangle. \quad \text{(A5)}$$

This is the expectation value of the potential energy of one degree of freedom. The expectation value for one degree of freedom in a classical-harmonic system is $k_B T/2$.

The total kinetic energy (KE) in the real and phonon spaces is given by

$$\mathrm{KE} = \sum_i \frac{1}{2}\frac{|\mathbf{p}_i|^2}{m_i} = \sum_k \frac{1}{2}\dot{S}_k^* \dot{S}_k. \quad \text{(A6)}$$

As the kinetic energy of a particle in a classical system is proportional to the square of the magnitude of its momentum (and no higher order terms), this expression for the kinetic energy is valid in anharmonic systems. The classical-harmonic expectation value of the mode kinetic energy is $k_B T/2$.

In a classical-harmonic system there is an equipartition of energy between all degrees of freedom, so that the average kinetic energy of a mode will be equal to its average potential energy. Thus,

$$\langle E_k \rangle_{\mathrm{harm}} = \omega_k^2 \langle S_k^* S_k \rangle = k_B T. \quad \text{(A7)}$$

The instantaneous energy in a given mode predicted by Eqs. (A4) and (A6) is readily calculated in the MD simulations. As discussed elsewhere, it is the quasi-harmonic mode frequencies that should be used in these calculations.[6]

*Electronic address: kaviany@umich.edu

[1] A. J. H. McGaughey and M. Kaviany, Phys. Rev. B **69**, 094303 (2004).

[2] M. Asen-Palmer, K. Bartkowski, E. Gmelin, M. Cardona, A. P. Zhernov, A. V. Inyushkin, A. Taldenkov, V. I. Ozhogin, K. M. Itoh, and E. E. Haller, Phys. Rev. B **56**, 9431 (1997).

[3] J. Callaway, Phys. Rev. **113**, 1046 (1959).

[4] G. P. Srivastava, *The Physics of Phonons* (Adam Hilger, Bristol, 1990).

[5] J. Li, Ph.D. thesis, Massachusetts Institute of Technology, Cambridge, MA, 2000.

[6] A. J. H. McGaughey, Ph.D. thesis, University of Michigan, Ann Arbor, MI, 2004.

[7] J. Li, L. Porter and S. Yip, J. Nucl. Mater. **255**, 139 (1998).

[8] Y. H. Lee, R. Biswas, C. M. Soukoulis, C. Z. Wang, C. T. Chan, and K. M. Ho, Phys. Rev. B **43**, 6573 (1991).

[9] N. W. Ashcroft and N. D. Mermin, *Solid State Physics* (Saunders College Publishing, Fort Worth, 1976).

[10] A. J. H. McGaughey and M. Kaviany, Int. J. Heat Mass Transfer **47**, 1783 (2004).

[11] J. Ziman, *Electrons and Phonons* (Oxford University Press, Oxford, 2001).

[12] M. T. Dove, *Introduction to Lattice Dynamics* (Cambridge University Press, Cambridge, England, 1993).

[13] P. K. Schelling, S. R. Phillpot, and P. Keblinski, Appl. Phys. Lett. **80**, 2484 (2002).

[14] P. K. Schelling and S. R. Phillpot, J. Appl. Phys. **93**, 5377 (2003).

[15] S. Sinha, P. K. Schelling, S. R. Phillpot, and K. E. Goodsen, J. Appl. Phys. **97**, 023702 (2005).

[16] J. Michalski, Phys. Rev. B **45**, 7054 (1992).

[17] C. Oligschleger and J. C. Schon, Phys. Rev. B **59**, 4125 (1999).

[18] A. H. Nayfey and D. T. Mook, *Nonlinear Oscillations* (Wiley, New York, 1979).

[19] V. L. Gurevich, *Transport in Phonon Systems* (North-Holland, Amsterdam, 1986).

[20] A. A. Maradudin, in *Dynamical Properties of Solids*, Volume 1, edited by G. K. Horton and A. A. Maradudin (Elsevier, New York, 1974), pp. 1–82.